Modelling of pseudoplastic deformation of carbon/carbon composites with a pyrocarbon matrix

2008 Modelling Simul. Mater. Sci. Eng. 16 055001

(http://iopscience.iop.org/0965-0393/16/5/055001)

Modelling Simul. Mater. Sci. Eng. **16** (2008) 055001 (18pp) doi:10.1088/0965-0393/16/5/055001

Modelling of pseudoplastic deformation of carbon/carbon composites with a pyrocarbon matrix

V Shavshukov[1], A Tashkinov[1], Y M Strzhemechny[2,4] and D Hui[3]

[1] Department of Composite Materials and Structures Mechanics, Perm State Technical University, 29 Komsomolsky Av., Perm, 614000, Russia
[2] Department of Physics and Astronomy, Texas Christian University, TCU Box 298840, Fort Worth, TX 76129, USA
[3] Department of Mechanical Engineering, University of New Orleans, New Orleans, LA 70148, USA

E-mail: Y.Strzhemechny@tcu.edu

Received 11 December 2007, in final form 2 April 2008
Published 14 May 2008
Online at stacks.iop.org/MSMSE/16/055001

Abstract

An engineering micromechanical model for carbon/carbon composites with a pyrocarbon (PC) matrix is presented. The model of the matrix plays an essential role in modelling of the material. This model takes into account the structural heterogeneity of the PC matrix and the anisotropy of the carbon fibres. The PC matrix is considered as a polycrystalline aggregate of anisotropic PC grains (or crystallites) with random shapes and orientations. The carbon fibres are homogeneous and anisotropic. The mathematical foundation for the model is a homogenization procedure for a multicomponent heterogeneous medium with a stochastic structure, anisotropic components and variable volume fractions of the components. The stochastic structure of the matrix generates fields of fluctuating microstresses and stochastic fractures of individual PC grains. Due to the anisotropy, the PC grains can fracture or become partially damaged via several fracture modes with different probabilities depending on the macrostress state of the material. The model allows calculation of the full stress–strain diagram for the carbon/carbon composite with arbitrary multiaxial loads and to forecast the appropriate strength limits. As an application of the model, numerical results are presented for a three-point bending of a short beam made of unidirectional materials. The calculated interlaminar shear strength matches the available experimental data.

1. Introduction

Carbon/carbon (C/C) fibre composites with a pyrolytic carbon matrix grown by chemical vapour deposition (CVD) or infiltration (CVI) techniques are materials of great importance

[4] Author to whom any correspondence should be addressed.

for industrial applications due to their unique properties. The fibres and the matrix of these composites exhibit significantly different strength and deformability. For instance, carbon fibre surpasses the pyrocarbon (PC) matrix in tensile strength (see section 5) by two orders of magnitude and in tensile elongation by a factor of six or more. Besides, the PC matrix is highly defective and contains a large number of cracks and pores. Thus it seems that the matrix damage and the fracture behaviour have to crucially affect the mechanical response of the composite material. To simulate the deformation and fracture of these composites on the basis of micromechanics, we have to know the elastic and fracture properties of the matrix and the carbon fibres. The properties of the fibre are rather well known. As far as the matrix is concerned, the C/C composites have one feature that distinguishes them noticeably from other fibre composites. The PC matrix is deposited into a prefabricated reinforcing fibre preform (filament substrate) by a CVD or a CVI process and does not exist independently of the preform. Therefore, it is not possible to measure directly the mechanical properties of the matrix on standard samples and to use these data in micromechanical models of the composite. One solution of this problem is to simulate the matrix behaviour on the basis of the structural characteristics of the matrix (which can be studied by optical or electron microscopes, x-ray structural analysis, etc) and the properties of the carbon phases.

Mechanical behaviour of the C/C composites with a PC matrix has been extensively studied experimentally since the 1970s (when the composites were first developed). A crucial observation in these experiments was that the C/C composites exhibit a nonlinear pseudoplastic behaviour under deformation whereas their constitutive components are brittle. The full stress–strain diagrams for these composites often have descending parts indicating damage in materials' components. It was understood that these mechanical features are determined by a complex microstructure of the material and the matrix. A number of experimental studies were performed on the relationship between the microstructure and the mechanical properties. The first micromechanical descriptions of the C/C composites were based on simple models, which considered the carbon matrix as a homogeneous medium analogous to polymer matrix composites [1]. In recent years, a number of papers have been published with the heterogeneity of the PC matrix taken into account [2–6]. These models allowed calculation of the effective elastic moduli of the matrix and the material and described their dependence on the volume fractions of fibres, pores and structural characteristics of the material. However, fracture processes in the matrix were not taken into consideration. Here we present a model which takes into account the anisotropy and the multimode failures of the PC matrix grains, and predicts the strength properties of the C/C composites.

2. Model of the PC matrix

A CVD-grown PC matrix is a complex aggregate of various carbon phases—turbostratic carbon, crystalline graphite, amorphous carbon, etc—and pores. In [7], all types of PCs are divided into three categories—rough laminar, smooth laminar and isotropic. The rough laminar is the most crystallographically perfect type. In heat-treated composites, the volume fraction of this type of PC is considerably more abundant than the others. All the carbon phases consist of grains, or crystallites, of various shapes and sizes with a hexagonal (or amorphous) crystallographic and a hexagonal (or isotropic) elastic symmetry of each individual grain. For simplicity we will assume that the initial strainless PC matrix consists only of rough laminar-type crystallites, which we will designate below as undamaged (perfect). The presence of grains of another carbon phase can be easily introduced into the model.

Hence, we suggest the following model of a PC matrix [8]. It represents a multicomponent heterogeneous medium consisting of PC grains with a hexagonal crystallographic symmetry and pores. The hexagonal crystallographic symmetry yields a transverse isotropic elastic symmetry of the grains. The shapes and sizes of the grains and pores, as well as the orientations of the elastic symmetry axes of the grains are random. The mutual shape and orientation correlation of adjacent grains is given in this model by appropriate correlation tensors.

The elastic moduli tensor C_{ijkl} of a PC crystallite has five independent components. In the crystallographic coordinate system $\{x_1, x_2, x_3\}$ (i.e. system with the coordinate axis x_3 as the hexagonal symmetry axis) this tensor has the following form:

$$C^{\mathrm{o}}_{ijmn} = a\delta_{ij}\delta_{mn} + b(\delta_{im}\delta_{jn} + \delta_{in}\delta_{jm}) + \gamma\delta_{i3}\delta_{j3}\delta_{m3}\delta_{n3} + \kappa(\delta_{i3}\delta_{j3}\delta_{mn} + \delta_{ij}\delta_{m3}\delta_{n3}) + \rho(\delta_{in}\delta_{j3}\delta_{m3} + \delta_{i3}\delta_{n3}\delta_{jm} + \delta_{im}\delta_{j3}\delta_{n3} + \delta_{i3}\delta_{m3}\delta_{jn}), \tag{1}$$

where the upper index 'o' refers to the crystallographic coordinate system, δ_{ik} is the Kronecker symbol and a, b, γ, κ and ρ are the elastic constants of the crystallite. These constants can be expressed in terms of technical elastic constants of a transversely isotropic medium: Young's moduli E_1, E_3, shear moduli G_{12}, G_{13} and Poisson's ratio ν_{13} in the x_1–x_3 plane.

For clarity, we will use the usual matrix layout of the C^{o}_{ijmn} tensor as follows:

$$C^{\mathrm{o}}_{ijmn} = \begin{pmatrix} c_{11} & c_{12} & c_{13} & 0 & 0 & 0 \\ c_{12} & c_{11} & c_{13} & 0 & 0 & 0 \\ c_{13} & c_{13} & c_{33} & 0 & 0 & 0 \\ 0 & 0 & 0 & c_{44} & 0 & 0 \\ 0 & 0 & 0 & 0 & c_{44} & 0 \\ 0 & 0 & 0 & 0 & 0 & c_{66} \end{pmatrix}, \tag{2}$$

where we use these notations:

$$c_{11} = C^{\mathrm{o}}_{1111},\ c_{12} = C^{\mathrm{o}}_{1122},\ c_{13} = C^{\mathrm{o}}_{1133},$$
$$c_{44} = 2C^{\mathrm{o}}_{2323},\ c_{66} = (C^{\mathrm{o}}_{1111} - C^{\mathrm{o}}_{1122})/2.$$

Under a deformation of the medium as a whole, any grain can be damaged or fractured. Each separate PC crystallite is a single crystal with a graphite-like structure. Graphite crystals such as pyrographite and quasimonocrystals of PC (see section 5) are brittle. Therefore, we accept that the fracture behaviour of the PC grains is elastic brittle. In the phenomenological fracture mechanics it is assumed that brittle solids fracture via rupture and shear modes. According to the symmetry of the grains, a fracture in a crystallographic system is possible through one of the following modes: a rupture along the x_3 axis, a rupture in any perpendicular direction, a shear in any plane parallel to the x_3 axis and in a perpendicular plane. For these fracture modes we have to formulate certain fracture criteria. We use the simplest phenomenological fracture criteria for anisotropic brittle materials in a crystallographic system in the Coulomb–Mohr form: any PC grain at a given stress state σ_{ij} fails if

$$\sigma_{33} \geqslant \sigma_3^+, \tag{3}$$

$$\sqrt{\sigma_{13}^2 + \sigma_{23}^2} \geqslant \tau_{13}, \tag{4}$$

$$(\sigma_{11} + \sigma_{22})/2 + \sqrt{(\sigma_{11} - \sigma_{22})^2/4 + \sigma_{12}^2} \geqslant \sigma_1^+, \tag{5}$$

$$\sqrt{(\sigma_{11} - \sigma_{22})^2/4 + \sigma_{12}^2} \geqslant \tau_{12}. \tag{6}$$

Here σ_3^+ and σ_1^+ denote tensile strengths in the x_3 and x_1 directions, τ_{13} and τ_{12}—shear strengths in planes x_1–x_3 and x_1–x_2, respectively.

After failure under any of the criteria (3)–(6), a grain loses a corresponding mechanical resistance mode but others remain. We assume that after such a failure, the grains continue to deform elastically, with elastic tensor components changing their values at the moment of fracture in a stepwise manner.

After fracture under criteria (3) and (4), a grain does not resist tension along the x_3 axis and shear in the x_1–x_3 and x_2–x_3 planes but continues to resist tension in any direction in the x_1–x_2 plane and shear in this plane. We will label all physical variables related to such partially damaged grains by an upper index '(1)'. In any strain state, the values of the stress components in these damaged grains have to be $\sigma_{33}^{(1)} \leqslant 0$ and $\sigma_{13}^{(1)} = 0$, $\sigma_{23}^{(1)} = 0$. For damaged grains we will use constitutive equations in the form of Hooke's law and select such elastic tensor components $C_{ijkl}^{(1)}$ that yield this type of mechanical resistance.

Let us consider for example a strain state of a$^{(1)}$-type damaged crystallite with tensions along the crystallographic axes $\varepsilon_{11}^{(1)} > 0$, $\varepsilon_{22}^{(1)} > 0$, $\varepsilon_{33}^{(1)} > 0$, and $\varepsilon_{13}^{(1)} \neq 0$, $\varepsilon_{23}^{(1)} \neq 0$. The first requirement mentioned above, $\sigma_{33}^{(1)} = C_{1133}^{(1)}\varepsilon_{11}^{(1)} + C_{1133}^{(1)}\varepsilon_{22}^{(1)} + C_{3333}^{(1)}\varepsilon_{33}^{(1)} \leqslant 0$, corresponds to $C_{1133}^{(1)} = C_{3333}^{(1)} = 0$, and the second requirement $\sigma_{13}^{(1)} = C_{1313}^{(1)}\varepsilon_{13}^{(1)} = 0$, $\sigma_{23}^{(1)} = C_{2323}^{(1)}\varepsilon_{23}^{(1)} = 0$ corresponds to $C_{1313}^{(1)} = C_{2323}^{(1)} = 0$. Thus, the elastic tensor $C_{ijmn}^{(1)}$ in this strain state has to have the following form:

$$C_{ijmn}^{\mathrm{o}(1)+} = \begin{pmatrix} c_{11} & c_{12} & 0 & 0 & 0 & 0 \\ c_{12} & c_{11} & 0 & 0 & 0 & 0 \\ 0 & 0 & 0 & 0 & 0 & 0 \\ 0 & 0 & 0 & 0 & 0 & 0 \\ 0 & 0 & 0 & 0 & 0 & 0 \\ 0 & 0 & 0 & 0 & 0 & c_{66} \end{pmatrix}, \tag{7}$$

where an additional upper index '+' refers to positive values of a normal strain $\varepsilon_{11}^{(1)} > 0$, $\varepsilon_{22}^{(1)} > 0$, $\varepsilon_{33}^{(1)} > 0$.

In other strain states with tension along the x_3 axis and compression in the x_1–x_2 plane, e.g. $\varepsilon_{33}^{(1)} > 0$, $\varepsilon_{11}^{(1)} < 0$, $\varepsilon_{22}^{(1)} < 0$, the second requirement $\sigma_{13}^{(1)} = \sigma_{23}^{(1)} = 0$ yields $c_{2323}^{(1)} = 0$. The first requirement $\sigma_{33}^{(1)} = C_{1133}^{(1)}\varepsilon_{11}^{(1)} + C_{1133}^{(1)}\varepsilon_{22}^{(1)} + C_{3333}^{(1)}\varepsilon_{33}^{(1)} \leqslant 0$, or in this case $\varepsilon_{33}^{(1)}C_{3333}^{(1)}/C_{1133}^{(1)} - (|\varepsilon_{11}^{(1)}| + |\varepsilon_{22}^{(1)}|) \leqslant 0$, does not allow to choose unambiguously the values of $C_{1133}^{(1)}$ and $C_{3333}^{(1)}$ for a damaged crystallite. However, for PC $C_{3333}^{(1)}/C_{1133}^{(1)} = 2.1$ (see section 5) and hence in such a state the tension deformation $\varepsilon_{33}^{(1)} > 0$ has to be accompanied by a compression deformation in the x_1–x_2 plane that is twice as large. Therefore, such strain states have a low statistical weight (a low probability of occurring in a stochastic medium) and in simple examples below are not realized. So we accept that in any state with $\varepsilon_{33}^{(1)} > 0$, a PC crystallite of a$^{(1)}$-type damage has the form (7).

Now let us consider a strain state of a$^{(1)}$-type damaged crystallite with compressions along the crystallographic axes $\varepsilon_{11}^{(1)} < 0$, $\varepsilon_{22}^{(1)} < 0$, $\varepsilon_{33}^{(1)} < 0$, and $\varepsilon_{13}^{(1)} \neq 0$, $\varepsilon_{23}^{(1)} \neq 0$. In this state, the requirement $\sigma_{33}^{(1)} = C_{1133}^{(1)}\varepsilon_{11}^{(1)} + C_{1133}^{(1)}\varepsilon_{22}^{(1)} + C_{3333}^{(1)}\varepsilon_{33}^{(1)} \leqslant 0$ is true exactly and the requirement $\sigma_{13}^{(1)} = \sigma_{23}^{(1)} = 0$ corresponds to $C_{2323}^{(1)} = 0$. Therefore, the elastic tensor $C_{ijmn}^{(1)}$ in this strain

state has to have the form

$$C^{o(1)-}_{ijmn} = \begin{pmatrix} c_{11} & c_{12} & c_{13} & 0 & 0 & 0 \\ c_{12} & c_{11} & c_{13} & 0 & 0 & 0 \\ c_{13} & c_{13} & c_{33} & 0 & 0 & 0 \\ 0 & 0 & 0 & 0 & 0 & 0 \\ 0 & 0 & 0 & 0 & 0 & 0 \\ 0 & 0 & 0 & 0 & 0 & c_{66} \end{pmatrix}, \tag{8}$$

where the upper index '−' denotes compression. Similarly, consideration of mixed states with compression along the x_3 axis but tension in the x_1–x_2, plane, i.e. $\varepsilon^{(1)}_{33} < 0$, $\varepsilon^{(1)}_{11} > 0$, $\varepsilon^{(1)}_{22} > 0$, allows us to choose the elastic tensor of a$^{(1)}$-type damaged crystallite for states with $\varepsilon^{(1)}_{33} < 0$ in the form (8).

Thus the elastic moduli tensor of a$^{(1)}$-type damaged crystallite for any strain state can be written in the form:

$$C^{o(1)}_{ijmn} = C^{o(1)+}_{ijmn} H(\varepsilon^{(1)}_{33}) + C^{o(1)-}_{ijmn}[1 - H(\varepsilon^{(1)}_{33})], \tag{9}$$

where $H(\varepsilon^{(1)}_{33})$ is the impulse function, which is equal to 1 when $\varepsilon^{(1)}_{33} \geqslant 0$ and equal to zero otherwise, and tensors $C^{o(1)+}_{ijmn}$, $C^{o(1)-}_{ijmn}$ are determined by equations (7) and (8). The elastic tensor $C^{o(1)}_{ijmn}$ from (9) is a function of strain $\varepsilon^{(1)}_{33}$.

After fracture of a PC crystallite under criteria (5) and (6) the crystallite does not resist tension along any direction in the x_1–x_2 plane and shear in this plane but continues to resist tension along the x_3 axis and shear in any plane parallel to this axis. We will label such physical crystallites with an upper index '(2)'. Similarly to the above discussion, analysis of possible mechanical resistance modes of a crystallite damaged in such a way allows to choose its elastic moduli tensor in the form

$$C^{o(2)}_{ijmn} = C^{o(2)+}_{ijmn} H(\varepsilon^{(2)}_{33}) + C^{o(2)-}_{ijmn}[1 - H(\varepsilon^{(2)}_{33})], \tag{10}$$

where

$$C^{o(2)+}_{ijmn} = \begin{pmatrix} 0 & 0 & 0 & 0 & 0 & 0 \\ 0 & 0 & 0 & 0 & 0 & 0 \\ 0 & 0 & c_{33} & 0 & 0 & 0 \\ 0 & 0 & 0 & c_{44} & 0 & 0 \\ 0 & 0 & 0 & 0 & c_{44} & 0 \\ 0 & 0 & 0 & 0 & 0 & 0 \end{pmatrix}, \tag{11}$$

$$C^{o(2)-}_{ijmn} = \begin{pmatrix} c_d & c_d & c_{13} & 0 & 0 & 0 \\ c_d & c_d & c_{13} & 0 & 0 & 0 \\ c_{13} & c_{13} & c_{33} & 0 & 0 & 0 \\ 0 & 0 & 0 & c_{44} & 0 & 0 \\ 0 & 0 & 0 & 0 & c_{44} & 0 \\ 0 & 0 & 0 & 0 & 0 & 0 \end{pmatrix}, \; c_d \equiv (c_{11} + c_{12})/2. \tag{12}$$

After fracture under all the criteria (3)–(6), the crystallite resists only a uniform hydrostatic compression.

The elastic tensor of a PC matrix as a whole, $C_{ijmn}(\vec{r})$, when the matrix contains all types of crystallites, in a global coordinate system will take the form:

$$C_{ijmn}(\vec{r}) = \sum_{k=0}^{2} \lambda_k(\vec{r}) C^{o(k)}_{pqrs} \alpha_{ip}(\vec{r}) \alpha_{jq}(\vec{r}) \alpha_{mr}(\vec{r}) \alpha_{ns}(\vec{r}), \tag{13}$$

where $\lambda_k(\vec{r})$ is an indicator of a k-type crystallite, i.e. $\lambda_k(\vec{r}) = 1$ within this crystallite and is equal to zero otherwise. $C^{o(k)}_{pqrs}$ are defined by (2), (9), (10) and $\alpha_{ip}(\vec{r})$ are the directional cosines of the local crystallographic coordinate axes of a crystallite at point $\vec{r}$ relative to the global coordinate system.

Elastic tensor $C_{ijmn}(\vec{r})$ is a function of the $\vec{r}$ coordinate and the strain state of the medium through (9) and (10).

3. Stochastic boundary value problem for polycrystalline PC matrix

To describe a macroscopic behaviour of the PC matrix we make a standard assumption [16] that there exists the so-called representative (or reference) volume element (RVE) with dimensions much greater than the crystallite sizes but much smaller than other characteristic dimensions of the system and such that the stresses and strains averaged over the RVE volume are smooth functions of the coordinates in the body. These averaged stresses $\langle \sigma_{ij}(\vec{r}) \rangle$ and strains $\langle \varepsilon_{ij}(\vec{r}) \rangle$ are related via the effective elastic moduli

$$\langle \sigma_{ij}(\vec{r}) \rangle = C^*_{ilkl} \langle \varepsilon_{kl}(\vec{r}) \rangle, \tag{14}$$

where angular brackets indicate volume averaging over RVE, i.e. $\langle \sigma_{ij}(\vec{r}) \rangle = 1/V \int_V \sigma_{ij}(\vec{r})\, \mathrm{d}\vec{r}$, and analogously for $\langle \varepsilon_{ij}(\vec{r}) \rangle$. The effective elastic moduli are derived through homogenization of the boundary value problem. For the case of a PC matrix, this problem has to be formulated for a multicomponent medium with variable volume fractions of its components.

The boundary value problem consists of equilibrium and constitutive equations

$$\begin{aligned} &\nabla_j \sigma_{ij}(\vec{r}) = 0, \\ &\sigma_{ij}(\vec{r}) = C_{ijmn}(\vec{r}) \varepsilon_{mn}(\vec{r}), \\ &\varepsilon_{mn}(\vec{r}) = [\nabla_m u_n(\vec{r}) + \nabla_n u_m(\vec{r})]/2, \qquad \nabla_m \equiv \frac{\partial}{\partial r_m}, \end{aligned} \tag{15}$$

where $\varepsilon_{ij}(\vec{r})$, $\sigma_{ij}(\vec{r})$ are the strain and stress tensors, $u_i(\vec{r})$ is a displacement vector. The boundary conditions we take in the form of fixed displacements $u_i(\vec{r})$ on the external surface Γ of the medium defined by equation $u_i(\vec{r})|_{\vec{r}\in\Gamma} = \varepsilon^*_{ij} r_j$, where ε^*_{ij} is some constant tensor. The use of such boundary conditions implies that the volume-averaged strains are homogeneous in the problem region $\langle \varepsilon_{ij}(\vec{r}) \rangle = \varepsilon^*_{ij}$ (but the actual strains $\varepsilon_{ij}(\vec{r})$ are heterogeneous). These conditions are simple but sufficient for obtaining effective properties [9, 11]. The volume of the medium confined by the Γ surface has to be equal or greater than RVE.

Tensor $C_{ijmn}(\vec{r})$ is a stochastic function of $\vec{r}$. It is constant within each crystallite and changes stepwise when going to another crystallite due to the change in the crystallite type and the rotation of the crystallographic axes. Thus, the boundary value problem (15) is a stochastic one. The differential equations of the boundary problem (15) can be transformed into an integral equation for strains by a common procedure (e.g. [9, 11])

$$\varepsilon_{ik}(\vec{r}) = \varepsilon^*_{ik} + \int_V \mathrm{d}\vec{r}_1 G_{ip,qk}(\vec{r} - \vec{r}_1) C'_{pqmn}(\vec{r}_1) \varepsilon_{mn}(\vec{r}_1). \tag{16}$$

where $G_{pq,rs}$ is Green's tensor function for a generic (reference) homogeneous medium. The choice of a generic medium is arbitrary but in our case it is convenient to

choose this medium as an isotropic homogeneous medium with an elastic tensor $\langle C_{ijkl}\rangle$ because then $C'_{pqmn}(\vec{r})$ in (16) is $C'_{pqmn}(\vec{r}) \equiv C_{pqmn}(\vec{r}) - \langle C_{pqmn}\rangle$ with a mean value $\langle C'_{pqmn}(\vec{r})\rangle = 0$. The prime symbol here and below indicates fluctuations of a given quantity.

A formal solution of (16) can be obtained in the form of perturbation series in powers of fluctuations $C'_{pqmn}(\vec{r})$ by an iteration procedure. As of today, there are no exact results on the convergence of this series and the appropriate series for the effective elastic moduli that are derived from (16) by a homogenization procedure. Neglecting fluctuations C'_{pqmn} in (16) yields the Voigt approximation. Our earlier calculations for the effective elastic moduli of a polycrystalline PC [10] show that the first order approximation (in fact, for the effective moduli it is a second order in C'_{pqmn} as the term with the first power in C'_{pqmn} disappears after homogenization) and the self-consistent approximation yields close results—with a difference of about 7%. In [10] it is also shown that the results of these calculations meet rigorous Hashin–Shtrinkman bounds. As shown in [11], the self-consistent approximation is equivalent to a summation over a certain infinite subseries of the full perturbation series. Thereby we can expect that at least the series for the effective moduli is fast convergent. Dutta *et al* [12] performed calculations of the effective moduli for several different polycrystals in the first and second orders and found that the results differ by only 6%. They also concluded that the series for the effective moduli of polycrystals converges fast. We will assume that the series for $\varepsilon_{ik}(\vec{r})$ also converges fast and will confine them by the first order in calculations to follow.

Thus, in the first order approximation, the solution for the strains is

$$\varepsilon_{ik}(\vec{r}) = \varepsilon^*_{ik} + \int_V \mathrm{d}\vec{r}_1 G_{ip,qk}(\vec{r} - \vec{r}_1) C'_{pqmn}(\vec{r}_1)\varepsilon^*_{mn}(\vec{r}_1) \tag{17}$$

and for the stresses

$$\sigma_{ij}(\vec{r}) = \left\{ C_{ijmn}(\vec{r}) + C_{ijpq}(\vec{r}) \int_V \mathrm{d}\vec{r}_1 G_{pr,sq}(\vec{r} - \vec{r}_1) C'_{rsmn}(\vec{r}_1) \right\} \varepsilon^*_{mn}. \tag{18}$$

Solution (18) for $\sigma_{ij}(\vec{r})$ is a very complex stochastic function of $\vec{r}$ due to a complicated dependence on the $C_{pqmn}(\vec{r})$ tensor on $\vec{r}$. Full description of the stochastic variable requires knowledge of the probability distribution densities or a full set of the statistical moments of the variable. For macroscopic specimens of the medium, and for the case when the averaged strains $\langle\varepsilon_{ij}\rangle$ and stresses $\langle\sigma_{ij}\rangle$ vary slowly, we can apply a homogenization procedure and instead of considering the stochastic function $\sigma_{ij}(\vec{r})$, we proceed to its statistical moments, i.e. the mean values of the stress fluctuations products of the $\langle\cdots\sigma'_{ij}\sigma'_{mn}\sigma'_{pq}\cdots\rangle$ type, where $\sigma'_{ij}(\vec{r}) \equiv \sigma_{ij}(\vec{r}) - \langle\sigma_{ij}(\vec{r})\rangle$. We will calculate moments of the first and the second orders only and will neglect higher moments in accordance with the arguments provided above.

Thus, we introduce

$$\langle\sigma_{ij}(\vec{r})\rangle \equiv \frac{1}{V}\int \sigma_{ij}(\vec{r})\,\mathrm{d}\vec{r}, \tag{19}$$

$$\langle\sigma'_{ij}(\vec{r})\sigma'_{mn}(\vec{r})\rangle \equiv \frac{1}{V}\int \sigma'_{ij}(\vec{r})\sigma'_{mn}(\vec{r})\,\mathrm{d}\vec{r}. \tag{20}$$

Here V is the volume of the specimen, i.e. the volume of the region for the boundary problem (15). Equation (19) deals with mean stresses, and equation (20) with the correlations of the stress fluctuations.

Substitution of (18) into (19) and (20) yields

$$\langle\sigma_{ij}\rangle = \left\{\langle C_{ijmn}\rangle + \int_V \mathrm{d}\vec{r}\, G_{pr,sq}(\vec{r}) K^{ijpq}_{rsmn}(\vec{r})\right\}\varepsilon^*_{mn} \tag{21}$$

$$\begin{aligned}\langle\sigma'_{ij}\sigma'_{mn}\rangle = \Bigg\{ & K^{ij\alpha\beta}_{mn\gamma\delta}(0) + \langle C_{ijpq}\rangle \int_V \mathrm{d}\vec{r}\, G_{pr,sq}(\vec{r}) K^{rs\alpha\beta}_{mn\gamma\delta}(\vec{r}) + \langle C_{mnpq}\rangle \int_V \mathrm{d}\vec{r}\, G_{pr,sq}(\vec{r}) K^{ij\alpha\beta}_{rs\gamma\delta}(\vec{r}) \\ & + \langle C_{ijpq}\rangle\langle C_{mntu}\rangle \int_V \mathrm{d}\vec{r}\,\mathrm{d}\vec{r}_1 G_{pr,sq}(\vec{r}) K^{rs\alpha\beta}_{vw\gamma\delta}(\vec{r}-\vec{r}_1) G_{tv,wu}(\vec{r}_1)\Bigg\}\varepsilon^*_{\alpha\beta}\varepsilon^*_{\gamma\delta},\end{aligned} \tag{22}$$

where $K^{ijpq}_{rsmn}(\vec{r}) \equiv \langle C'_{ijpq}(r_1) C'_{rsmn}(r_2)\rangle$ is the elastic moduli correlation tensor of 8th rank and $\vec{r} = \vec{r}_1 - \vec{r}_2$.

The expression inside the braces in (21) gives the effective elastic moduli tensor of the medium in the used approximation:

$$C^*_{ijmn} = \langle C_{ijmn}\rangle + \int_V \mathrm{d}\vec{r}\, G_{pr,sq}(\vec{r}) K^{ijpq}_{rsmn}(\vec{r}).$$

The correlation tensor $K^{ijpq}_{rsmn}(\vec{r})$ depends on the geometrical structure of the material (i.e. shapes and sizes of grains), orientations of the crystallographic axes of grains and correlations of these quantities for adjacent grains, (i.e. the texture of the material), and can be calculated for a particular material by means of e.g. Monte-Carlo simulation. In this model the $K^{ijpq}_{rsmn}(\vec{r})$ tensor describes the structure of the material. Solutions (17) and (18) assume that the fluctuations are small so we can neglect the third and higher statistical moments.

Statistical moments (21) and (22) characterize the stress field in the medium as a whole. In order to investigate fracture of different crystallites we need the values of these quantities within each type of crystallites, i.e. to go from the so-called unconditional moments to conditional statistical moments, which define the stress field inside crystallites of a particular type. To do this let us point out that the stress tensor can be written as

$$\sigma_{ij}(\vec{r}) = \sum_{k=0}^{2} \sigma^{(k)}_{ij}(\vec{r})\lambda_k(\vec{r}), \tag{23}$$

where $\sigma^{(k)}_{ij}(\vec{r})$ denotes the stress field within a subset of k-type crystallites.

Multiplying (23) by $\lambda_k(\vec{r})$ and taking into account that $\lambda_k(\vec{r})\lambda_l(\vec{r}) = \delta_{kl}$ we obtain

$$\sigma^{(k)}_{ij}(\vec{r})\lambda_k(\vec{r}) = \sigma_{ij}(\vec{r})\lambda_k(\vec{r}). \tag{24}$$

We will introduce into (24) indicator fluctuations $\lambda'_k(\vec{r}) = \lambda_k(\vec{r}) - \langle\lambda_k(\vec{r})\rangle \equiv \lambda_k(\vec{r}) - p_k$, where p_k is a volume fraction of k-type crystallites, and perform averaging over the entire volume of the material. Averaging of the left side of (24) gives

$$\langle\sigma^{(k)}_{ij}(\vec{r})\lambda_k(\vec{r})\rangle \equiv \frac{1}{V}\int_V \sigma^{(k)}_{ij}(\vec{r})\lambda_k(\vec{r})\,\mathrm{d}\vec{r} = \frac{1}{V}\int_{V_k} \sigma^{(k)}_{ij}(\vec{r})\,\mathrm{d}\vec{r},$$

where V_k is the volume of the part of the material containing only k-type crystallites. On the other hand, averaging only over the area of k-type crystallites, which we denote here and below by a subscript k, is by definition

$$\langle\sigma^{(k)}_{ij}(\vec{r})\rangle_k \equiv \frac{1}{V_k}\int_{V_k} \sigma^{(k)}_{ij}(\vec{r})\,\mathrm{d}\vec{r}.$$

The latter averaging gives us mean stresses in k-type crystallites. Taking into account an obvious relation $p_k = V_k/V$, we have

$$\langle\sigma^{(k)}_{ij}(\vec{r})\lambda_k(\vec{r})\rangle = p_k\langle\sigma^{(k)}_{ij}(\vec{r})\rangle_k.$$

Thus, we obtain the following exact formula for the first conditional statistical moment of $\sigma_{ij}^{(k)}(\vec{r})$ (mean stresses in a k-type crystallite):

$$\langle\sigma_{ij}^{(k)}\rangle_k = \langle\sigma_{ij}\rangle + \frac{1}{p_k}\langle\lambda_k'(\vec{r})\sigma_{ij}'(\vec{r})\rangle. \tag{25}$$

Inserting $\sigma_{ij}'(\vec{r}) \equiv \sigma_{ij}(\vec{r}) - \langle\sigma_{ij}(\vec{r})\rangle$ from (18) into (25) and neglecting the third order moments we obtain

$$\begin{aligned}\langle\sigma_{ij}^{(k)}\rangle_k &= \langle\sigma_{ij}\rangle + \frac{1}{p_k}\left\{L_{ij\alpha\beta}^{(k)}(0) + \langle C_{ijpq}\rangle\int \mathrm{d}\vec{r}_1 G_{pr,sq}(\vec{r}_1)L_{rs\alpha\beta}^{(k)}(\vec{r}_1)\right\}\varepsilon_{\alpha\beta}^*,\\ L_{rs\alpha\beta}^{(k)}(\vec{r}) &\equiv \langle\lambda_k'(\vec{r}_1)C_{rs\alpha\beta}'(\vec{r}_2)\rangle, \quad \vec{r} = \vec{r}_1 - \vec{r}_2.\end{aligned} \tag{26}$$

The $L_{rs\alpha\beta}^{(k)}(\vec{r})$ statistical moment in (26) as well as the correlation tensor $K_{rsmn}^{ijpq}(\vec{r})$ mentioned above can be calculated for a particular material by some numerical simulation techniques.

Similar considerations lead to the following exact expression for the second conditional statistical moment of the stresses $\sigma_{ij}^{(k)}(\vec{r})$—correlations of the stress fluctuations inside a k-type crystallite:

$$\langle\sigma_{ij}'^{(k)}\sigma_{mn}'^{(k)}\rangle_k = \langle\sigma_{ij}'\sigma_{mn}'\rangle - \frac{1}{p_k^2}\langle\lambda_k'(\vec{r})\sigma_{ij}'(\vec{r})\rangle\langle\lambda_k'(\vec{r})\sigma_{mn}'(\vec{r})\rangle + \frac{1}{p_k}\langle\lambda_k'(\vec{r})\sigma_{ij}'(\vec{r})\sigma_{mn}'(\vec{r})\rangle. \tag{27}$$

Once again, we have to neglect the last third order term and, as was done in equation (26), we can reduce (27) to

$$\begin{aligned}\langle\sigma_{ij}'^{(k)}\sigma_{mn}'^{(k)}\rangle_k = \langle\sigma_{ij}'\sigma_{mn}'\rangle - \frac{1}{p_k^2}\Bigg\{&\left[L_{ij\alpha\beta}^{(k)}(0) + \langle C_{ijpq}\rangle\int \mathrm{d}\vec{r}_1 G_{pr,sq}(\vec{r}_1)L_{rs\alpha\beta}^{(k)}(\vec{r}_1)\rangle\right]\varepsilon_{\alpha\beta}^*\\ &\times\left[L_{mn\gamma\delta}^{(k)}(0) + \langle C_{mntu}\rangle\int \mathrm{d}\vec{r}_2 G_{tv,wu}(\vec{r}_2)L_{vw\gamma\delta}^{(k)}(\vec{r}_2)\right]\varepsilon_{\gamma\delta}^*\Bigg\}.\end{aligned} \tag{28}$$

The statistical moments (21), (22), (26) and (28) give essential but incomplete information about the random stress fields $\sigma_{ij}(\vec{r})$ and $\sigma_{ij}^{(k)}(\vec{r})$. To fully characterize these random fields, the probability distribution densities of these fields are needed. The two statistical moments (21), (22) or (26), (28) do not allow unambiguous reconstruction of the probability distribution. In any case, the values of $\sigma_{ij}^{(k)}(\vec{r})$ at a given macroscopic strain are limited to finite ranges. Therefore the distribution densities of $\sigma_{ij}^{(k)}$ have to be functions defined in a finite range of arguments. The lower limit of this range is the minimal possible value of $\sigma_{ij}^{(k)}$ and the upper limit is the maximum possible value of $\sigma_{ij}^{(k)}$. These maximum and minimum are unknown *a priori* and are the solutions of the boundary value problem (15). A rigorous reconstruction of the distribution density function is a separate task. We can draw some conclusions about a possible form of this distribution density by using the Voigt approximation for the boundary problem (15). Within this approximation, the strains are homogeneous throughout the body $\varepsilon_{ij}(\vec{r}) = \varepsilon_{ij}^*$, and the stochastic stresses are $\sigma_{ij}^{(k)}(\vec{r}) = \alpha_{ip}(\vec{r})\alpha_{jq}(\vec{r})\alpha_{mr}(\vec{r})\alpha_{ns}(\vec{r})C_{pqrs}^{\mathrm{o}(k)}\varepsilon_{rs}^*$, where only the directional cosines $\alpha_{ip}(\vec{r})$ are stochastic variables. For random orientations of the crystallographic axes of a crystallite a simple Monte-Carlo simulation shows that the probability density for $\sigma_{ij}^{(k)}$ is quasirectangular (within the Voigt approximation). Here, intending to provide an engineering model of the material, we will approximate the actual probability distribution density for $\sigma_{ij}^{(k)}(\vec{r})$ with a rectangular distribution, regarding it as a trial distribution. This rectangular distribution has two parameters, which are the marginal values of its argument. For the case of the $\sigma_{ij}^{(k)}(\vec{r})$ field, they have to represent the minimum and the maximum values of the stress components within k-type crystallites, which occur

throughout the medium at a given macroscopic strain. The trial and the actual distributions will match each other best if they have a maximum number of coinciding statistical moments. We have only two statistical moments for the actual distribution (26) and (28). So, to select the two unknown parameters of the rectangular distribution, we will make a reasonable assumption of choosing them in a way that the first and the second statistical moments of this distribution coincide with (26) and (28), respectively. We also assume that the medium is macroscopically homogeneous and macroscopically isotropic. In this case, the probability distribution of the $\sigma_{ij}^{(k)}(\vec{r})$ field does not depend on the $\vec{r}$ coordinate.

Thus, we reconstruct the probability distribution density $f(\sigma_{ij}^{(k)})$ of each separate field component $\sigma_{ij}^{(k)}$ in the form:

$$f(\sigma_{ij}^{(k)}) = \begin{cases} \dfrac{1}{a_{ij}^{(k)} - b_{ij}^{(k)}}, & \text{when} \quad a_{ij}^{(k)} \leqslant \sigma_{ij}^{(k)} \leqslant b_{ij}^{(k)}, \\ 0, & \text{otherwise}, \end{cases} \tag{29}$$

and

$$a_{ij}^{(k)} = \langle \sigma_{ij}^{(k)} \rangle - \sqrt{3\langle \sigma_{ij}^{\prime(k)^2} \rangle},$$

$$b_{ij}^{(k)} = \langle \sigma_{ij}^{(k)} \rangle + \sqrt{3\langle \sigma_{ij}^{\prime(k)^2} \rangle},$$

where $\langle \sigma_{ij}^{(k)} \rangle$ and $\langle \sigma_{ij}^{\prime(k)^2} \rangle$ are given by (26) and (28). It is easy to verify by integrating (29) that the first and the second statistical moments of the $\sigma_{ij}^{(k)}$ stresses coincide with (26) and (28), i.e.

$$\int \sigma_{ij}^{(k)} f(\sigma_{ij}^{(k)}) \, \mathrm{d}\sigma_{ij}^{(k)} = \langle \sigma_{ij}^{(k)} \rangle,$$

and

$$\int [\sigma_{ij}^{(k)} - \langle \sigma_{ij}^{(k)} \rangle]^2 f(\sigma_{ij}^{(k)}) \, \mathrm{d}\sigma_{ij}^{(k)} = \langle \sigma_{ij}^{\prime(k)^2} \rangle.$$

The $a_{ij}^{(k)}$ and $b_{ij}^{(k)}$ variables give us approximately the minimum and the maximum stresses within accepted assumptions.

The joint probability distribution density for the two field components $\sigma_{ij}^{(k)}$ and $\sigma_{mn}^{(k)}$, for the case when i, j and m, n are not equal pairwise, is determined by the two-dimensional rectangular distribution density $f(\sigma_{ij}^{(k)}, \sigma_{mn}^{(k)})$. The two-dimensional domain $\Re$ of variation for its arguments $\sigma_{ij}^{(k)}$ and $\sigma_{mn}^{(k)}$ is chosen in a way that covariation of $f(\sigma_{ij}^{(k)}, \sigma_{mn}^{(k)})$ will coincide with (28):

$$\int_{\Re} \sigma_{ij}^{\prime(k)} \sigma_{mn}^{\prime(k)} f(\sigma_{ij}^{(k)}, \sigma_{mn}^{(k)}) \, \mathrm{d}\sigma_{ij}^{(k)} \, \mathrm{d}\sigma_{mn}^{(k)} = \langle \sigma_{ij}^{\prime(k)} \sigma_{mn}^{\prime(k)} \rangle. \tag{30}$$

Here, we do not provide an explicit expression for the density $f(\sigma_{ij}^{(k)}, \sigma_{mn}^{(k)})$ because it is too cumbersome. The details of reconstruction of the two-dimensional rectangular distribution can be found in [13] and elsewhere. The three-dimensional even distribution density $f(\sigma_{ij}^{(k)}, \sigma_{mn}^{(k)}, \sigma_{pq}^{(k)})$ can be constructed in a very similar manner. The higher-dimensional distributions will not be used here because the fracture criteria (3)–(6) include only up to three different stress components.

The expressions (21), (22), (26) and (28) together with the reconstructed distribution densities (29), etc give the solution of the stochastic boundary value problem (15) for a PC matrix. This solution is used to model the deformation and fracture processes in the following section.

4. Deformation and fracture of a PC matrix

Due to the stochastic structure of the matrix, deformation, damage and fracture processes in the matrix are stochastic as well.

In the proposed model it is assumed that the stress state of the medium at given macroscopic strain is achieved as a result of a stepwise increase in the macroscopic strain from zero to a given value with a small step. At each step, different crystallites may become damaged or fractured with certain probabilities. At small macroscopic strains ε^*_{ij}, the $a^{(k)}_{ij}$ and $b^{(k)}_{ij}$ margins from (29) are small and all the possible values of $\sigma^{(k)}_{ij}(\vec{r})$ throughout the matrix do not match any fracture criteria (3)–(6) for all the types of crystallites. Therefore there is no damage in the matrix at such macroscopic strains. After increasing the macroscopic strain to a certain value, one or several fracture criteria for some crystallites are fulfilled and a certain amount of damage occurs for a specific amount of proper crystallites. For instance, if a certain quantity of the 0-type crystallites fractures under the criterion (3) they become 1-type crystallites. Thus, the volume fraction p_0 of the 0-type (undamaged) decreases and the volume fraction p_1 of the 1-type (partially damaged) crystallites increases. The volume fractions of different crystallites change and the effective elastic moduli tensor C^*_{ijmn} of the matrix changes, respectively.

Let us label the fracture probability of a k-type crystallite under a ξth criterion as $\pi_{k\xi}$. The first index k in $\pi_{k\xi}$ enumerates the type of a crystallite. It varies from 0 to 2. The second index ξ represents the fracture criterion. It varies from 1 to 4. The value $\xi = 1$ corresponds to fracture under the criterion (3), $\xi = 2$ corresponds to fracture under the criterion (4), $\xi = 3$ to the criterion (5) and $\xi = 4$ to the criterion (6).

It is easy to write the formulae for probabilities $\pi_{k\xi}$. An appropriate probability is determined by an integral of the probability density $f(\sigma^{(k)}_{ij})$, $f(\sigma^{(k)}_{ij}, \sigma^{(k)}_{mn})$ or $f(\sigma^{(k)}_{ij}, \sigma^{(k)}_{mn}, \sigma^{(k)}_{pq})$ for a k-type crystallite over a domain restricted by a ξth fracture criterion. For example, the fracture probability of a 0-type crystallite under the criterion (3)—fracture due to a tension rupture along the x_3 axis—is given by the expression:

$$\pi_{01} = \int_{\sigma^{(0)}_{33} \geqslant \sigma^+_3} f(\sigma^{(0)}_{33})\, \mathrm{d}\sigma^{(0)}_{33}. \tag{31}$$

Other $\pi_{k\xi}$ are defined by equivalent formulae.

Fracture probabilities allow calculation of the volume fractions of different types of crystallites at a given step of deformation per known volume fractions at a previous step. Let us label the volume fraction p_k at an N-step of the macroscopic strain as $p_k|_N$. A simple combinatorial analysis leads to the following relations between the volume fractions at an N-step and a previous $(N-1)$-step:

$$\begin{aligned}
p_0|_N &= p_0|_{N-1}(1-\pi_{01})(1-\pi_{02})(1-\pi_{03})(1-\pi_{04}),\\
p_1|_N &= p_1|_{N-1}(1-\pi_{13})(1-\pi_{14}) + p_0|_{N-1}[1-(1-\pi_{11})(1-\pi_{12})](1-\pi_{13})(1-\pi_{14}),\\
p_2|_N &= p_2|_{N-1}(1-\pi_{21})(1-\pi_{22}) + p_0|_{N-1}[1-(1-\pi_{03})(1-\pi_{04})](1-\pi_{01})(1-\pi_{02}),\\
p_3|_N &= 1 - p_0|_N - p_1|_N - p_2|_N.
\end{aligned} \tag{32}$$

The meaning of the equations in (32) is obvious. The first equation in (32) indicates that the volume fraction of undamaged 0-type grains at an N-step of a macroscopic strain is equal to a product of the same fraction at an $(N-1)$-step, and the probability of these grains not becoming damaged under any criterion. The second equation specifies that the volume fraction of 1-type damaged grains at an N-step is equal to a sum of two terms of an $(N-1)$-step. The first term is a product of volume fraction of 1-type damaged grains that existed already at an $(N-1)$-step and the probability of these grains not becoming damaged. The second term is a

product of a volume fraction of undamaged 0-type grains at an $(N-1)$-step and probability of a damage conversion of these crystallites into 1-type damaged grains only. The third equation in (32) is completely equivalent to the second one. The fourth equation in (32) gives a volume fraction of fully fractured crystallites and pores.

The entry conditions at the $N = 0$ step for the iterative process (32) are determined by the state of the matrix before deformation. If in this initial condition the matrix consists only of undamaged 0-type crystallites and pores then the entry conditions are $p_0|_{N=0} = 1 - \Pi$, $p_1|_{N=0} = 0$, $p_2|_{N=0} = 0$ and $p_3|_{N=0} = \Pi$, where Π is the initial porosity of the matrix.

The model is implemented as an iterative algorithm with a stepwise varying external parameter, the macroscopic strain ε^*_{ij}. At each step, the boundary value problem (15) is solved as described above. So, the statistical moments of the stress fields, the probabilities of crystallite fracture, the volume fractions of all the types of crystallites and the effective elastic moduli of the medium are calculated at each step of the macroscopic deformation. The values of all these quantities at a previous step are the entry conditions for the next step of iteration.

The described algorithm plays the role of nonlinear constitutive equations for a PC matrix. It describes the mechanical behaviour of the matrix at an arbitrary deformation path in a 6-dimensional strain space.

5. Numerical results

To use the described algorithm in calculations of the full deformation curve for the PC matrix we employ elastic and strength properties of a PC crystallite from [14, 15]. These properties were measured on macroscopic specimens of PC deposited on a perfect flat substrate so that the graphene planes were parallel to the substrate. Such specimens are quasisingle crystals of PC. The temperature of deposition was 1100 °C, the same as in the case of a PC matrix deposition into a preform of a carbon fibre to produce a C/C composite. The inter-planar spacing of a graphite structure d_{003}, the main parameter controlling the properties of these structures was also the same in both cases.

The strength properties of a PC crystallite are

$$\sigma_1^+ = 31.8\,\text{MPa}, \quad \sigma_3^+ = 5.0\,\text{MPa}, \quad \tau_{13} = 5.0\,\text{MPa}, \quad \tau_{12} = 32.8\,\text{MPa}. \tag{33}$$

The technical elastic constants of a PC crystallite are

$$E_1 = 29.5\,\text{GPa}, \quad E_3 = 10.5\,\text{GPa}, \quad G_{12} = 15.0\,\text{GPa}, \quad G_{13} = 2.3\,\text{GPa}, \quad \nu_{13} = 0.44, \tag{34}$$

where E_1 and E_3 are the Young moduli in the x_1 and x_3 directions, G_{12} and G_{13} are the shear moduli and ν_{13} is the Poisson ratio.

The components of the elastic moduli tensor from (2), which correspond to the technical constants from (34), are

$$\begin{aligned} &c_{11} = 34.2\,\text{GPa}, \quad c_{12} = 4.32\,\text{GPa}, \quad c_{13} = 5.80\,\text{GPa} \\ &c_{33} = 12.2\,\text{GPa}, \quad c_{44} = 2.30\,\text{GPa}, \quad c_{66} = 15.0\,\text{GPa}. \end{aligned} \tag{35}$$

In this paper, to calculate the integrals in the expressions for the statistical moments (26) and (28) we used the simplest form of the elastic moduli correlation tensor

$$K^{ijpq}_{rsmn}(\vec{r}) = \langle C'_{ijpq}(0) C'_{rsmn}(0) \rangle \delta(\vec{r}), \tag{36}$$

where $\delta(\vec{r})$ is the Dirac impulse function. The correlation tensor (36) corresponds to a fully disordered polycrystal without any texture.

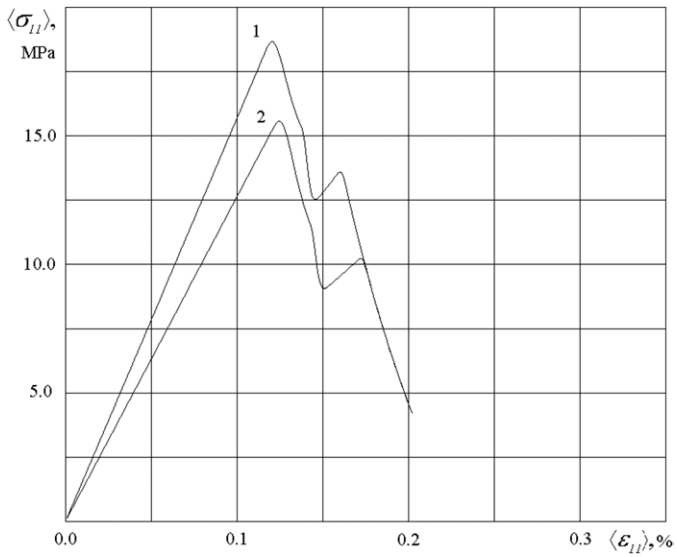

Figure 1. Uniaxial stress tension. Curve 1: 0% porosity, curve 2: 10% porosity.

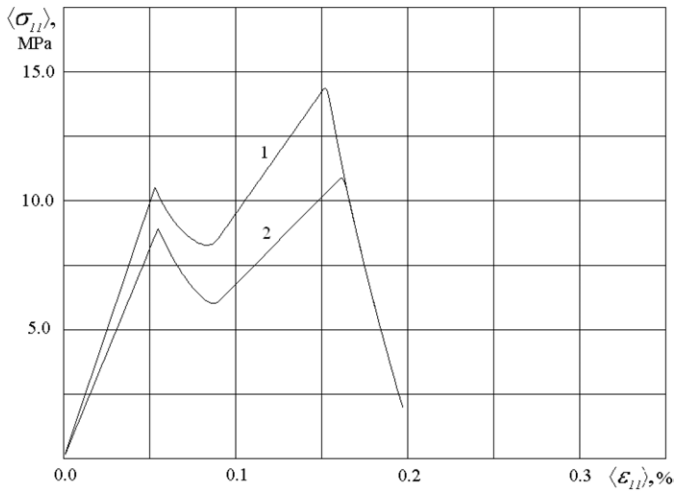

Figure 2. Uniaxial strain tension. Curve 1: 0% porosity, curve 2: 10% porosity.

Figures 1–4 represent the full deformation curves for the cases of a uniaxial stress tension, a uniaxial strain tension, a macroscopic shear and a proportional tri-axial (hydrostatic) tension.

All the deformation curves are nonlinear and have two local maxima. At strains that corresponded to the first local maxima, criteria (3) and (4) begin to match and the 1-type damaged PC grains appear. Progressively, the volume fraction of such damaged grains increases and at a local minimum all the grains are damaged in this way. Then the matrix deforms elastically up to the second local maxima when the fracture criteria (5) and (6) begin to match for the 1-type damaged PC grains. After this damage, a separate grain becomes fully fractured. Eventually, the mechanical resistance of the PC matrix deteriorates completely. The absolute maximum on each curve is the ultimate strength for the appropriate deformation path.

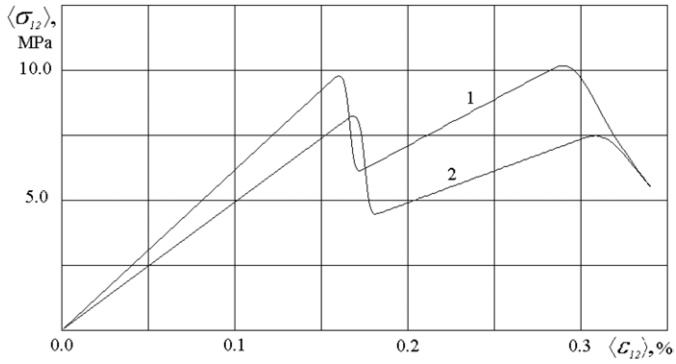

Figure 3. Macroscopic shear in the 1–2 planes. Curve 1: 0% porosity, curve 2: 10% porosity.

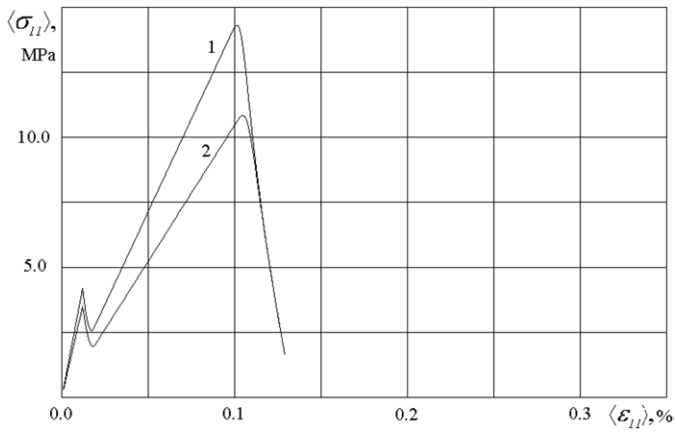

Figure 4. Proportional tri-axial (hydrostatic) tension. Curve 1: 0% porosity, curve 2: 10% porosity.

6. Modelling a unidirectional C/C composite

From a micromechanical point of view, a unidirectional composite is a multicomponent inhomogeneous material. As in the case of the matrix, we will describe this composite using effective properties derived through the homogenization procedure. To simplify the homogenization for the composite we assume that the characteristic size of heterogeneity of the material (in this case, the mean distance between the fibre yarns) is well above the characteristic size of heterogeneity of the matrix, i.e. the mean crystallite size. It is not always true; however it allows carrying out the homogenization of the material separately at two different levels of the size scale. At the first level, the homogenization is performed over a representative volume with linear sizes less than the mean distance between the yarns. After this homogenization the material is modelled as fibres embedded into a homogeneous matrix with effective properties calculated according to the algorithm from the previous sections. At the second level the homogenization is performed over a representative volume with dimensions much greater than the mean distance between the yarns. After the second homogenization the composite as a whole can be considered as a homogeneous material with effective properties.

The distribution of fibre centres in a cross-section perpendicular to the fibres is random. The matrix is a nonlinear medium and the properties of the matrix depend on the strains.

The iterative algorithm described above plays the role of the constitutive equations for the matrix. The fibres are elastically brittle up to the point of fibre fracture, so they obey Hooke's law.

We will apply the described model to the case of a three-point short beam bending of a unidirectional C/C composite specimen with fibres aligned along the beam axis.

According to the accepted assumptions, the effective homogenized medium is a homogeneous transversely isotropic with the transverse symmetry axis parallel to the fibre direction. There are several standard techniques to calculate the effective elastic properties of such medium. Here we use a well-known model for elastic moduli of fibre reinforced materials described in [18], which was further developed in [19] and is currently widely accepted [16]. For calculation of the effective properties this model considers each fibre of the composite as embedded into a layer of the matrix and this compound cylinder is placed into the effective homogeneous medium. This model provides simple formulae for the four effective elastic moduli of the medium E_1^*, E_2^*, G_{12}^*, ν_{12}^* (global coordinate axis x_1 is along the fibre direction) and somewhat more complicated formula for G_{23}^*. Formulae for E_1^*, E_2^*, G_{12}^*, ν_{12}^* provide very good results for these moduli with volume fractions of the fibres in a full range from 0 to 1. A formula for G_{23}^* provides a less accurate value for the shear modulus in the x_2–x_3 plane at a high fibre volume fraction; however, this modulus is not involved in the stress calculations for a beam under bending. Therefore, the four formulae mentioned above are sufficient to consider the mechanical response of the beam under bending.

We calculate a mechanical response of a short beam in a tree-point bending experiment according to the ASTM standard D-790-80. In this experiment, a straight beam with a square cross-section is positioned on two supports and is loaded at the centre of the specimen perpendicularly to the length of a beam. This experiment provides the interlaminar shear strength of the material when the ratio of the longitudinal and transverse dimensions of the beam specimen is chosen according to standard recommendations.

For computational modelling of the bending experiment, the beam specimen was chosen with a length of 25.2 mm and a square cross-section of $3.6 \times 3.6\,\text{mm}^2$, whereas the span between the points of support was 18.0 mm. So the length/span/thickness ratio for the specimen was 7 : 5 : 1 as prescribed by the D-790-80 standard for obtaining the interlaminar shear failure.

A standard finite element method (FEM) was used to calculate the strain and the stress fields in the specimen. In the initial state, before loading, the material of the specimen has homogeneous effective properties throughout the specimen volume. During the loading, the effective properties of the composite will vary continuously through the specimen volume when the matrix properties will change due to damages of the PC crystallites. In order to simplify calculations we substitute the continuous variation of the effective properties of the material with a stepwise variation. For this purpose the specimen is divided into plies parallel to fibres (and perpendicular to the loading direction) with thicknesses of 0.1028 mm. Thus, the specimen is divided into 35 plies. A simple bending theory states that stresses depend only on the transverse coordinate of the beam. Although we employ a precise 3D FEM calculation for stresses yielding stress concentrations and accounting for the local effects (supports, load application), for the effective elastic properties of the plies we assume dependence only on transverse coordinate and not on the longitudinal coordinate. Bending experiments on real short beams often reveal very localized crumpling (or indentation) damages near the supports and the loading point, where stress concentrations occur, but the final failure of the specimen always happens at the median surface (central ply) of the beam specimen. Hence, neglecting the longitudinal variation of plies' properties should not essentially influence the failure behaviour of the central ply, which is crucial in these experiments. The properties of each ply depend on

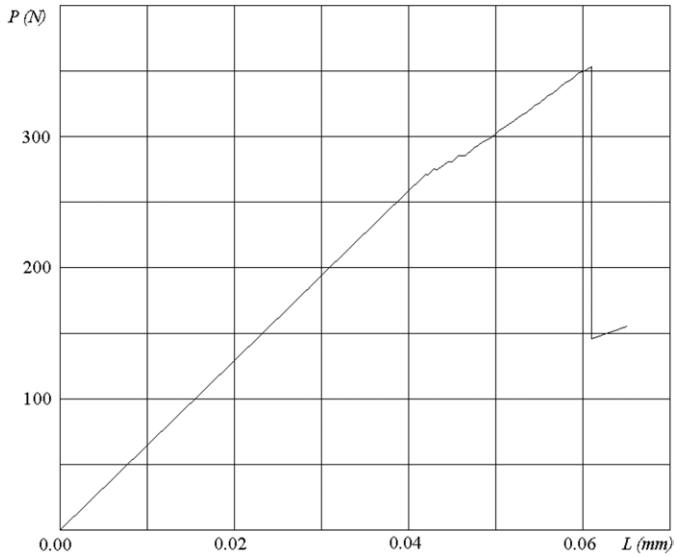

Figure 5. Three-point short beam bending of a unidirectional C/C specimen.

the strain state of the ply due to matrix damaging. The properties of a separate ply are assumed homogeneous throughout the ply volume and are determined by the mean strain of the ply. Therefore, here we neglect a variation of the elastic properties within an individual ply, and thus the ply thickness is taken to be very small. However, these properties change stepwise between adjacent plies with a small increment due to small ply thicknesses. These simplifications make calculations much faster because they substantially decrease the number of data exchanges between two computer codes—the FEM code and the PC matrix modelling code. The load applies at the centre of the specimen as the displacement of the fixed values varies stepwise from zero to the final value in small steps. At each loading step the global strain and stress fields throughout the whole specimen are calculated by an FEM for the properties of the plies. The effective moduli of a ply at a given mean ply strain are calculated as described above for the fibre moduli and the effective state-dependent moduli of the matrix in a given ply. The matrix moduli are calculated by the algorithm from section 4. Thus, the elastic properties of the plies vary nonlinearly with specimen deformation due to a nonlinear pseudoplastic behaviour of the matrix. The fibres do not fracture in this digital experiment since the calculated fibre stresses are much smaller than the appropriate fibre strength limits.

We used 'Torayca T-300'-like carbon fibre properties as follows:

$$E_1^f = 230\,\text{GPa}, \quad E_2^f = 14\,\text{GPa}, \quad G_{12} = 14\,\text{GPa}, \quad \nu_{12}^f = 0.23$$

(axis x_1 is along the fibres).

The volume fraction of the fibres in the composite was 63%. The initial total porosity of the PC matrix was taken to be 10%.

The calculated short beam bending diagram in coordinates 'applied force P(N) versus cross head displacement l (mm)' is presented in figure 5.

Up to a displacement of 0.042 mm no damage processes occur in the material and applied load increases linearly with deflection. After loading above this value, damage processes in the matrix related to the failure criteria (3) and (4) originate in the central ply of the beam. In the displacement range from 0.042 mm to 0.061 mm these damage processes progress and

the damage areas capture adjacent plies one after another. But there are no zones yet of a full fracture in the matrix throughout the whole volume of the beam specimen since no damage under the criteria (5) and (6) takes place. At displacements slightly greater than 0.061 mm a final fracture of the matrix happens in the central ply, the shear stiffness of this ply falls to zero, and the loading tug drops dramatically. This moment corresponds to the interlaminar shear fracture of the specimen. The interlaminar shear strength calculated for the maximum loading force as per ASTM D-790-80 for this case is equal to 19.3 MPa. The experimentally measured values of the interlaminar shear strength for the composites with a close fibre volume fraction lay in the range 16–25 MPa [17].

7. Conclusion

C/C composites are media of a very complex internal structure. The purpose of this work was to develop an engineering model fit for practical applications and analysis of deformation and fracture behaviour in C/C composites under any loading conditions. The model is based on a homogenization procedure for a heterogeneous medium with a stochastic structure and anisotropic components. The homogenization method was applied to two types of statistical ensembles—the medium as a whole and each material component separately. The latter yields statistical characteristics of the stress fields in the components. These characteristics are used to calculate the fracture probabilities of the components.

The model of a PC matrix as a polycrystalline aggregate plays a central role in the proposed problem. The matrix model takes into account the highly anisotropic elastic and strength properties of PC crystallites and a stochastic nature of the matrix structure. These two factors yield fluctuating stress fields and a stochastic fracture of PC grains. The model uses the simplest hypothesis for the elastic and fracture behaviour of a PC grain. On the other hand, it explains a nonlinear pseudoplastic deformation of unidirectional C/C composites, when the matrix fracture processes are crucial, and gives reasonable values for the interlaminar shear strength. The generalization of the model to the case of multidirectional composites is rather straightforward since they consist of unidirectional elements.

Acknowledgments

This work was supported by the Russian Foundation for Basic Research Grant 07-01-97619.

References

[1] Buckley J D and Edie D D 1993 *Carbon–Carbon Materials and Composites* (Park Ridge, NJ: Noyes)
[2] Reznik B, Guellali M, Gerthsen D, Oberacker R and Hoffmann M J 2002 *Mater. Lett.* **53** 14–9
[3] Piat R, Reznik B, Schnack E and Gerthsen D 2003 *Carbon* **41** 1851–64
[4] Piat R, Reznik B, Schnack E and Gerthsen D 2004 *Compos. Sci. Technol.* **64** 2015–20
[5] Tsukrov I, Piat R, Novak J and Schnack E 2005 *Mech. Adv. Mater. Struct.* **12** 43–54
[6] Piat R, Tsurkov I, Mladenov N, Verijenko V, Guellali M, Schnack E and Hoffmann M J 2006 *Compos. Sci. Technol.* **66** 2997–3003
[7] Oberlin A 2002 *Carbon* **40** 7–24
[8] Shavshukov V E and Tashkinov A A 2004 *Proc. 11th Int. Conf. on Composites/Nano Engineering (Hiton-Head Island, SC, USA)* p 669
[9] Torquato S 2002 *Random Heterogeneous Materials* (New York: Springer)
[10] Sokolkin Yu V, Tashkinov A A and Shavshukov V E 1993 *Struct. Compos. Mater.* **1** 37 (in Russian)
[11] Gubernatis J E and Krumhansl J A 1975 *J. Appl. Phys.* **46** 1875

[12] Dutta T, Ballabh T K and Middya T R 1993 *J. Phys. D: Appl. Phys.* **26** 667
[13] Feller W 1971 *An Introduction to Probability Theory and its Applications* (New York: Wiley)
[14] Ostrovskii V S, Virgilyev Yu S, Kostikov V I and Shipkov N N 1987 *Artificial Graphite* (Moscow: Metallurgy) (in Russian)
[15] Vyatkin S E 1967 *Nuclear Graphite* (Moscow: Atom) (in Russian)
[16] Christensen R 1979 *Mechanics of Composite Materials* (New York: Wiley)
[17] McAlister L and Lachman W 1983 *Handbook of Composites* vol 4, ed A Kelley and S T Mileiko (Amsterdam: Elsevier)
[18] Hashin Z and Rosen B W 1964 *J. Appl. Mech.* **31** 223
[19] Christensen R M and Lo K H 1979 *J. Mech. Phys. Solids* **27** 315